In-flight Landing Location Predictions using Ascent Wind Data for High Altitude Balloons

Conference Paper · March 2013

DOI: 10.2514/6.2013-1294

4 authors, including:

Travis Fields
University of Missouri - Kansas City
36 PUBLICATIONS **82** CITATIONS

SEE PROFILE

In-flight Landing Location Predictions using Ascent Wind Data for High Altitude Balloons

Travis D. Fields*, Milan J. Heninger†, Jeffrey C. LaCombe‡
and Eric L. Wang§
University of Nevada, Reno, Nevada, 89557, USA

This paper presents a hardware and software system in which the landing location of a balloon–payload system is continually predicted and improved. Initial prediction parameters are corrected by estimating flight parameters using GPS data. The focus of this study is on small (less than 10 kg payload) balloon systems. For these systems, flight missions typically have a duration of a few hours (minimal loitering at altitude) and descend after the balloon bursts at an altitude in the range of 15-30 km.

Prior to launch, weather predictions are typically used to predict the flight path and landing location of the balloon-payload system. The prediction accuracy greatly depends on the stability of wind data, as well as the accuracy in predicting the balloon ascent speed, balloon burst altitude, and parachute descent speed. Differences between the predicted and actual landing locations of 60 km are not atypical.

Rather than relying on the pre-flight predictions, the system developed here measures ascent/descent speeds and wind speed during the balloon's ascent. Unlike the pre-flight predictions, the system provides chase and recovery personnel with an accurate prediction of the landing location that is periodically updated as the mission progresses. During ascent, GPS data is logged to provide both actual ascent speed and up-to-date spatial and temporal wind data. The ascent speed along with the logged wind data and initial estimates of the parachute-payload flight characteristics (mass, parachute size, etc.) are used to correct the flight model up to the time of balloon burst. During descent, the actual descent speed is used to further enhance predictions as the mission progresses.

Results calculated from post-processing actual balloon flight GPS data validate the methodology developed. Prediction accuracy is improved from an average predicted landing location error of 36% of the traveled range prior to launch. At the balloon burst location, prediction quality improves to 3.5% of the total range traveled on average. Additionally, real-time, in-flight prediction results verify the ability to perform the in-flight prediction updates on-board a balloon using a microprocessor and off-the-shelf radio communication equipment.

Nomenclature

A_p	=	Parachute area
b	=	Subscript used to denote the time step at the balloon burst location
C_d	=	Parachute coefficient of drag
e	=	Distance between the predicted and actual landing locations
E	=	Normalized predicted landing location error
j	=	Subscript for the current time step when calculating the ascent phase of a balloon mission
m	=	Total parachute-payload mass

*Graduate Research Assistant, Mechanical Engineering, 1664 N Virginia St. MS 312, Reno, NV, and AIAA Member.
†Undergraduate Research Assistant, Mechanical Engineering, 1664 N Virginia St. MS 312, Reno, NV, and AIAA Member.
‡Associate Professor, Chemical and Materials Engineering, 1664 N Virginia St. MS 388, Reno, NV, and AIAA Member.
§Associate Professor, Mechanical Engineering, 1664 N Virginia St. MS 312, Reno, NV.

n	=	Subscript for the current time step when calculating the descent phase of a balloon mission
R	=	Range, distance between the balloon launch and landing locations
$SEOM$	=	Standard error of the normalized landing location mean
t_B	=	Elapsed time at balloon burst
t_D	=	Elapsed time after balloon burst (total flight time = $t_B + t_D$)
$\hat{\mathbf{w}}_x$	=	Easterly wind speed estimate for entire wind column
$\hat{\mathbf{w}}_y$	=	Northerly wind speed estimate for entire wind column
$[x_b, y_b, z_b]$	=	Balloon burst coordinates
$[x_i, y_i, z_i]$	=	Launch location coordinates
$\hat{\mathbf{z}}$	=	Altitude vector corresponding to wind speed estimates
$\hat{\dot{z}}_a$	=	Predicted ascent rate
$\hat{z}_{max}$	=	Predicted burst altitude
Δt	=	Time step
μ_E	=	Normalized predicted landing location error averaged over all data sets
$\rho(z_n)$	=	Atmospheric air density at altitude z_n
σ_E	=	Sample standard deviation of the normalized predicted landing location error

I. Introduction

High-altitude ballooning is currently used all over the world for applications ranging from small student built experiment flights, to reentry vehicle testing.[1] Prior to launch, trajectory predictions are computed using wind and balloon-payload flight characteristic prediction data. Wind prediction data is typically gathered from weather forecasting system data. Several prediction utilities have been developed to predict the ascent trajectory of a balloon mission which perform full dynamical and thermal simulations of the balloon flight path.[2,3,4,5] An online prediction utility has also been developed by the amateur ballooning community[6] in which the user inputs launch location, wind information, burst altitude, ascent rate, and descent rate. This utility has seen widespread use in the small (less than 10 kg payload) ballooning community, which is the focus of this study. All of these prediction utilities have limited accuracy dependent directly on the quality of the forecast wind data and input parameters, resulting in differences between predicted and actual landing location on the order of 20 km (dependent on burst altitude and wind conditions).

Four major types of pre-flight prediction errors have been observed during testing when using the online prediction utility. First, discrepancies between the predicted and actual balloon ascent rates can produce errors in trajectory predictions. Work has been done to improve the ascent path prediction by incorporating full dynamical and thermal simulations in conjunction with precision balloon fill equipment.[2] As this paper is specifically focused on the smaller ballooning community, having precise fill equipment is typically not feasible (especially in high surface wind environments). Similarly, differences between predicted and actual parachute descent rates affect the prediction accuracy. These errors specifically arise from uncertainties in the parachute-payload characteristics (mass and parachute C_d). Additional prediction errors accrue if the balloon bursts (for latex balloons) at an altitude different than the predicted altitude. Finally, the largest contributor in landing location prediction errors are differences between forecasted and actual winds. As atmospheric modeling continues to improve this error is reduced; however, it can still easily lead to errors of 60 km or more.

Rather than attempt to improve pre-flight prediction quality, a hardware/software system has been developed to capture real-time flight data and use it to improve the landing location prediction quality during the mission and transmit the new prediction to ground crews in real-time. As many ballooning teams rely on line of sight communications to recover the payloads, knowing where the payloads will land is of paramount importance in order to maintain communications. As a part of a software engineering project based course, students designed a software interface similar to the one described at Oregon Institute of Technology.[7] The system runs on a laptop on the ground, creating new calculations based on down-linked data. Ascent rate corrections were made; however, no corrections were made during the descent phase. Additionally, a laptop had to be connected to the payload communication system via wireless stream. By developing a hardware/software system that simply transmits the new predicted landing location onboard the

balloon greatly reduces any hardware needed on the ground (as communication can be done with standard amateur (ham) radios).

II. Hardware Development

As the system hardware must fly on a balloon payload, it must be lightweight, low cost, capable of performing the computing and storage needs of the software, and must communicate with ground crews wirelessly in real-time. This was achieved through designing a custom printed circuit board (PCB) outfitted to support an ATmega 328 processor (Arduino), 900 MHz RF modem (XBee), basic serial communications for interfacing with amateur (ham) radio telecommunication devices, and multiple I/O ports for interfacing with tertiary devices. These requirements were established in order to create a system familiar to the majority of the small scale ballooning community, while still allowing for future development to fit individual needs. The schematic outlining the structure of the hardware is shown in Figure 1.

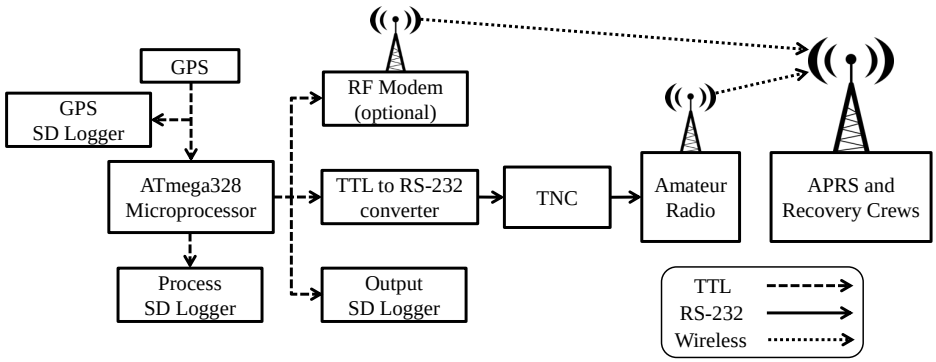

Figure 1: Schematic outlining major components and protocols used in the hardware system.

The ATmega microprocessor loaded with the Arduino firmware was utilized as it has many benefits over other processors. First, the Arduino platform is readily available and low cost, while offering extensive user support. Next, it is designed with numerous I/O ports in a small form factor specifically intended for prototype devices. Lastly, it is programmed in a simplified version of C, which most users will be familiar with or can quickly learn.

Communication requirements for the prediction system dictated that it use the most common protocols currently used by the ballooning community. This constraint left two major serial output protocols that needed to be supported, TTL (transistor-transistor logic) and recommended standard (RS) 232. For development, an Xbee RF modem for TTL and a terminal node controller (TNC) for RS-232 were chosen. Xbee's are small light weight radio systems that have a maximum range of over 20km, while not requiring special licensing by the end user. These radios permit simplified communication between multiple devices, including other payload or balloon systems, while still keeping power consumption and weight down. Concomitantly, RS-232 allows for communication between the prediction hardware and many other flight computer systems such as a TNC (e.g. Byonics TinyTrak) and similar microcomputers. These systems are most often used by teams employing amateur radio and APRS (Automatic Packet Recording System) to track their balloon payload systems. This configuration allows for much higher power radios, longer range, and more robust communications than RF modems, however they do require special licensing to use. The combined use of TTL and RS-232 based communication systems provides the end user with the ability to decide which radio transmission methods they wish to deploy, while offering little increase in the size or weight of the overall package.

Three micro SD card data loggers were also installed onboard the prediction hardware. In addition to simple data logging, these loggers have the added ability to read stored data. This allows for configuration and wind data files to be stored directly on the removable micro SD card. This prevents accidental modifications of the software, while requiring minimal training of people operating the system. The board can be easily configured to accept all common GPS systems, and allows for both actual and predicted GPS data to be readily shared with other devices in the payload system. These design considerations allow the hardware system to add significant functionality with minimal hardware changes to existing amateur ballooning

communication systems, maximizing its utility for ballooning teams and researchers. The fully constructed hardware board is shown in Figure 2.

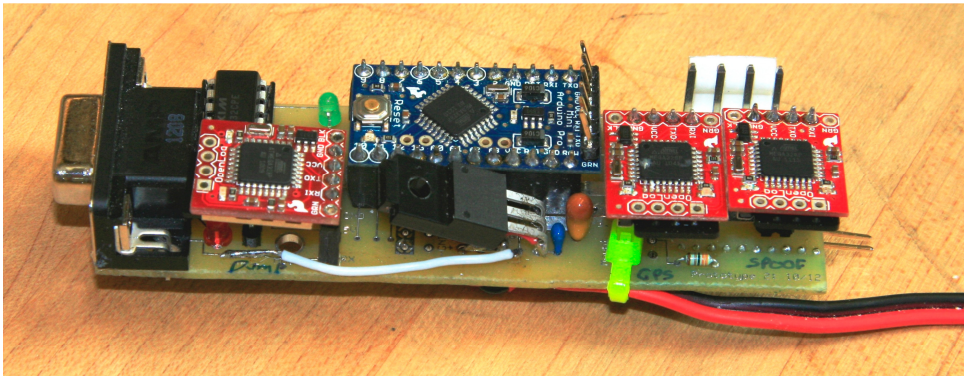

Figure 2: Fully assembled hardware PCB board.

As with all systems, there are certain limitations to the developed hardware. ATmega processors have limited onboard memory (≈4Kb RAM), which restricts program size and processing capabilities. Due to this memory restriction, predicated wind data is stored every 500 meters during the flight, while still permitting flight altitudes of 30km.

III. Algorithm Methodology

The prediction algorithm developed constantly updates the predicted landing location. At all times, the current location and altitude is used as the starting point for the prediction. During ascent, the actual ascent rate is measured and the horizontal wind speeds are stored thereby replacing initial forecasted winds. Wind speeds are recorded until balloon burst, at which time all the forecasted wind data has been replaced by wind data collected during the ascent. During descent, the descent rate is measured and used to determine the actual drag coefficient (C_d) of the parachute/payload system.

In order to compare the effectiveness of the various improvements applied, four milestones during a mission were selected (Figure 3). The first milestone is the pre-flight prediction, made just prior to launch. The second milestone (A) is after 25% of the time for the ascent phase. This milestone was selected to minimize the impact of the measured ascent winds (as this is better quantified at balloon burst) while still incorporating the measured ascent rate. The third milestone (B) is at balloon burst. The last milestone selected (C) occurs after 25% of the time for the descent phase (C) and includes the effects due to the updated descent rate profile.

The following sections outline the general prediction algorithm used to calculate the predicted landing location during the balloon mission. Additionally, details for the in-flight improvements are also discussed. The methods for testing the algorithm in simulation (using real-world GPS data) as well as full flight testing are also outlined.

A. General Prediction Algorithm

A generic flight path prediction algorithm is required prior to developing any in-flight prediction improvement system. In order to predict the landing location, several simulation input parameters are required (Table 1). For this study wind speeds are assumed to be only in the horizontal directions.

Starting with the launch location (x_i, y_i, z_i), the ascent phase can be calculated. As typical balloon ascent phases are nearly constant (as can be seen in Figure 3), the ascent rate used in path predictions is assumed to be constant. Additionally, the vehicle is assumed to always travel at the wind speed. Therefore, using zero-acceleration kinematics equations, the ascent flight path can be readily calculated.

$$x_j = x_{j-1} + \hat{\mathbf{w}}_x(j)\Delta t \tag{1}$$

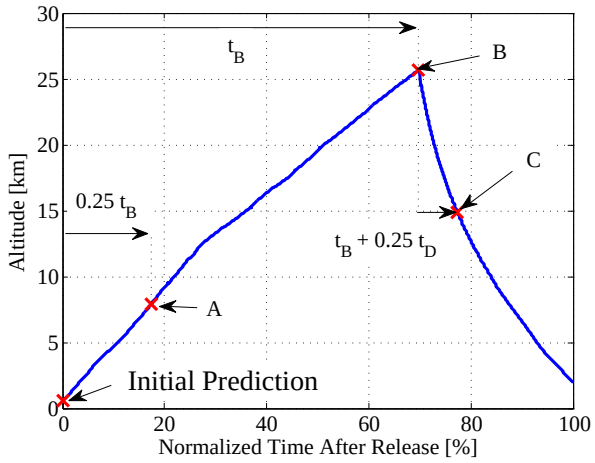

Figure 3: Visual depiction showing the four locations during each simulation where improvements are calculated.

A_p	Parachute area
C_d	Parachute coefficient of drag
m	Total payload mass
$[\hat{\mathbf{w}}_x, \hat{\mathbf{w}}_y, \hat{\mathbf{z}}]$	Predicted wind data set (typically from NOAA)
$[x_i, y_i, z_i]$	Launch location coordinates
$\hat{\dot{z}}_a$	Predicted ascent rate (constant)
$\hat{z}_{max}$	Predicted balloon burst altitude

Table 1: Input parameters required to calculate the predicted landing location.

$$y_j = y_{j-1} + \hat{\mathbf{w}}_y(j)\Delta t \tag{2}$$

$$z_j = z_{j-1} + \hat{\dot{z}}_a \Delta t \tag{3}$$

Where $(x_0, y_0, z_0) = (x_i, y_i, z_i)$, and j increments from $j = 1$. These equations are repeated until the altitude, z_j, reaches the predicted burst altitude. For convenience, the burst location is denoted by the index $j = b$, resulting in burst coordinates (x_b, y_b, z_b). Wind data is linearly interpolated to the current altitude, z_j, from the predicted wind data set. For this study Δt has been set to $10s$ in order to facilitate fast prediction computations with minimal loss in accuracy.

The descent phase is calculated in a similar manner, with the only change being the vertical speed is no longer assumed to be constant (as descent speed is dependent on air density). By assuming the parachute-payload system is traveling at terminal velocity, the velocity for a given time step (at a specific altitude) can be calculated.[8]

$$\dot{z}_n = -\sqrt{\frac{2mg}{\rho(z_n)A_pC_d}} \tag{4}$$

Using the descent speed and the predicted balloon burst location, the descent phase can be calculated in the same manner as the ascent phase.

$$x_n = x_{n-1} + \hat{\mathbf{w}}_x(n)\Delta t \tag{5}$$

$$y_n = y_{n-1} + \hat{\mathbf{w}}_y(n)\Delta t \tag{6}$$

$$z_n = z_{n-1} - \sqrt{\frac{2mg}{\rho(z_n)A_pC_d}}\Delta t \tag{7}$$

Where n increments from $n = b + 1$. This process is likewise repeated until the current altitude, z_n, has reached the predicted landing altitude. For this study, the predicted landing altitude is programmed to be the same as the launch altitude. This is necessary as the hardware system developed has limited memory and is unable to store ground altitudes for large areas; however, the altitude of the predicted landing location can be specified by the user when necessary.

In-flight landing location predictions utilize the same algorithm; however, the simulation initialization is modified to the balloon systems current location (whether it is ascending or descending). Once the vehicle has reached balloon burst, the ascent phase is simply not calculated as it is no longer applicable.

B. In-Flight Prediction Improvements

During ascent, wind data is collected every 500m from the GPS on-board the payload system (the interval is driven by the hardware limitations discussed in Sec. II). As this data is gathered, it is inserted into the stored array of wind data by replacing the forecasted data for the given altitude. As this collected data is gathered near the descent phase (both spatially and temporally), it will better represent what the payload-system will experience during the descent.

As discussed previously, for this work the balloon ascent rate is considered to be constant. After launch, the balloon-payload system often ascends at a rate different than predicted (typically because of errors in payload weights and/or free lift measurements). To reduce landing location prediction errors due to this discrepancy, the GPS data collected is used to perform a least squares linear fit of the ascent rate. This provides an estimate of the actual ascent speed, thereby improving the landing location prediction. A five point moving average is also used to further smooth the estimated ascent rate. Note: this smoothing was only applied to simulation results and had not been not implemented on the hardware at the time of full flight testing.

After burst, all prior error from ascent rate and burst altitude are no longer relevant and ascent collected wind data has completely replaced the forecast wind data; thus post burst predictions are subjected to predominantly descent rate estimation errors. Depending on the flight duration, there can still be significant errors due to changes in the wind conditions between ascent and descent; however, collecting wind data during the ascent provides the most accurate wind data available to the in-flight prediction algorithm. As the descent rate changes with altitude (due to changing air density), solving for a constant descent rate would not suffice; however, the drag force must remain constant if the system is falling at terminal velocity. Using a least-squares estimation of the descent rate, the corresponding drag coefficient can be calculated by rearranging Eq. 7.

$$\hat{C}_d = \frac{2mg}{\rho_n A_p \hat{\dot{z}}_n^2} \tag{8}$$

Using the new estimate of the drag coefficient, the descent path prediction can be recalculated. Since estimating the coefficient of drag relies on descent rate measurements (similar to the ascent rate estimation), the estimated descent rate is smoothed in order to reduce noise generated by numerically differentiating GPS altitude data. Like the ascent rate, smoothing of the descent rate data had not been implemented at the time of full flight testing.

C. Simulation Methodology

To facilitate comparing different balloon flight tests, the predicted landing location accuracies have been normalized. The normalized predicted landing location error, E, is defined as:

$$E = \frac{e}{R} \tag{9}$$

Where e is the distance between the actual and predicted landing location and R is the total distance traveled during the mission. Figure 4 provides a visual representation of the error between the predicted and actual landing locations, as well as a comparison of the downrange distance travelled and a projection of the actual flight path. As the prediction quality improves, the normalized landing location error will always approach

zero. In a similar fashion, the time after balloon release was also normalized by the total flight time. This yields a time array that starts at zero, and ends at 100%. These normalizations produce results than can be compared regardless of release altitude, ascent rate, payload mass or parachute size.

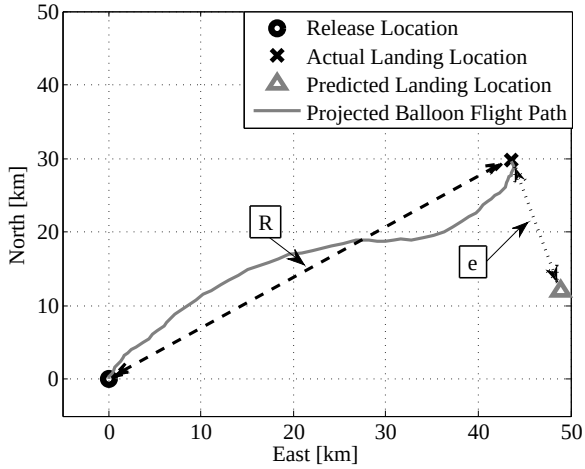

Figure 4: Projected view of the predicted landing location relative to the balloon flight path.

Results were computed from eleven different ballooning missions. Simulations were conducted by post-processing the collected GPS data. Two distinct mission types were tested, low altitude and high altitude. For each mission type the flight characteristics were nearly matched (ascent rate, payload weight, parachute size, etc.). NOAA forecast winds and best estimates for the other simulation parameters (Table 2) were used for simulation initialization.

Parameter	High Altitude	Low Altitude
A_p	$1.6m^2$	$1.6m^2$
C_d	1.0	1.0
m	$3.4kg$	$5.7kg$
$\hat{\dot{z}}_a$	$5.1m/s$	$5.1m/s$
$\hat{z_{max}}$	$15.2km$	$26.2km$

Table 2: Input parameters used during simulations for both high and low altitude balloon missions.

D. Experimental Verification

After the simulations were completed and the in-flight algorithm verified, the hardware system was flight tested on-board a balloon mission. For initial verification, flight tests were constrained to low altitudes. The national APRS communication frequency (144.390 MHz) was used so the ground crew could maintain communication even without line of sight (through the use of repeaters). The hardware was configured to alternate between transmitting its current location and predicted landing location. Transmissions were sent every one minute (although not every packet was successfully received). Internally, the hardware calculates a new predicted landing location approximately every 50 seconds and stores it to an internal flash memory card.

During each low-altitude test, two balloons were launched from the same location with approximately the same flight characteristics. Each balloon carried the in-flight prediction hardware; however, only one was transmitting to the ground crew at a time.

IV. Results

Results were compiled from the eleven ballooning missions at the four milestones discussed previously (Table 3). At each of the four locations, results were averaged over the eleven missions. Prior to balloon launch, predictions are only accurate to 36%. At balloon burst, the prediction accuracy has increased with a predictive error of 3.5% of the total range.

Prediction Location	$\mu_{\mathbf{E}}$	$\sigma_{\mathbf{E}}$	SEOM
Initial	36.07%	13.54%	1.23%
A	24.91%	10.90%	0.99%
B	3.53%	2.68%	0.24%
C	2.06%	1.05%	0.10%

Table 3: Average percent improvement over initial landing predictions for four locations during a balloon mission. (full flight predictor)

The prediction errors for four low altitude simulations are shown in Figure 5. Here the normalized prediction error as a function of normalized flight time are shown, demonstrating the improvement effects of the system throughout the flight. Tests 1 & 2 were collected from the same day using two balloons launched ten minutes apart. Tests 3 & 4 were also collected from two balloons launched on a different day with a five minute time separation between launch times. The average total distance traveled for low altitude test data was 47.6km, with a range of 41.6km to 53.5km. For tests 1 & 2, the normalized error steady decreases from about 45% to about 15% and remains there until the balloon bursts (at approximately 60% normalized flight time). For flights 3 & 4, the normalized error started small (i.e. a good prediction to start with) and states fairly constant until the balloon bursts. For all four tests, the normalized error drops to less than 5% immediately after burst.

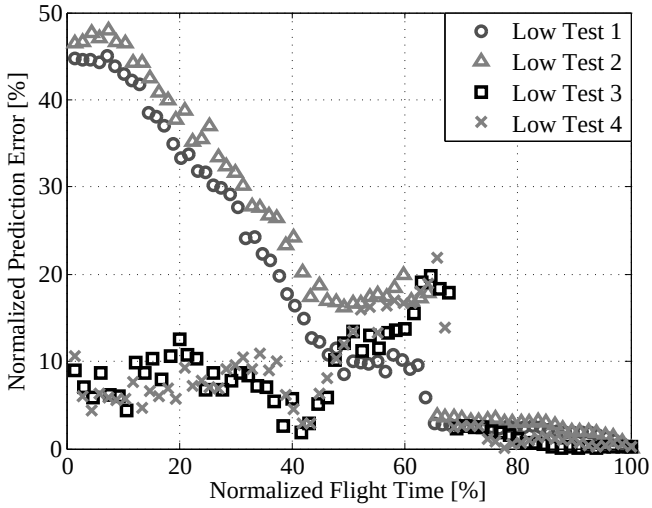

Figure 5: Landing location error computed from four different low altitude balloon missions.

The prediction errors for seven high altitude balloon mission simulations are shown in Figure 6. Tests 1-4 were collected during the same launch event using four balloons. Similarly, tests 5-7 were collected from the same launch event; however, tests 6 & 7 had much slower ascent rates than test 5. The average total distance traveled for high altitude test data was 120km, with a range of 97.1km to 174.7km. In all seven simulations, the predictions computed after burst show a normalized error of less than 10% .

Results have also been compiled for four ballooning missions in which the hardware was flown, calculating the predicted landing locations in real-time. These four missions correspond to the low altitude simulation results presented in Figure 5; however, the results presented in Figure 7 were calculated on the hardware discussed in Section II. As mentioned previously, at the time of testing smoothing of the ascent and descent

rates had not been implemented yet. The benefit of smoothing is particularly visible when comparing simulation and flight tests for low altitude flight tests 3 & 4 (see Figures 5 and 7).

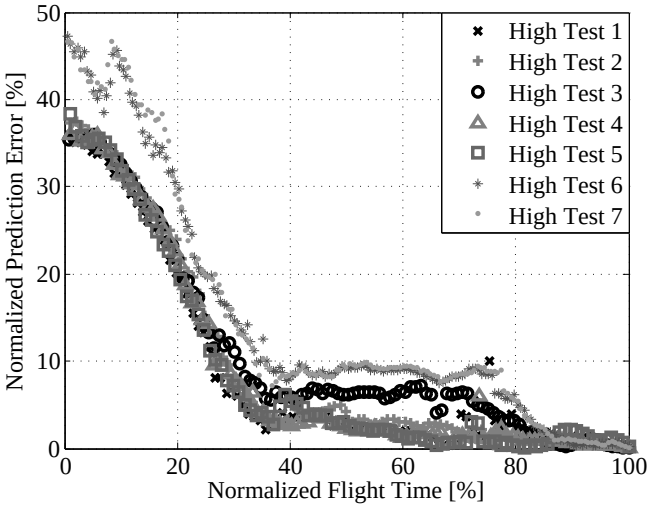

Figure 6: Landing location error computed from seven different high altitude balloon missions.

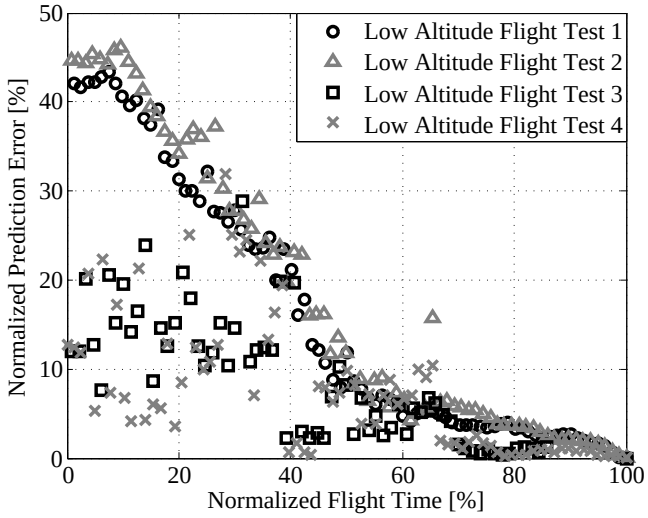

Figure 7: Landing location error calculated in real-time on-board the balloon-payload system.

As a final verification, a high altitude flight test was performed in which the in-flight prediction system reached 28.9km. The predicted landing locations throughout the flight are shown in Figure 8. Similarly to the low altitude flight testing, the smoothing algorithms had not yet been implemented. This can be clearly seen from the noise in prediction error during the ascent. The noise was further increased as the balloon ascent rate was significantly less ($\approx 3\ m/s$) than predicted .

V. Discussion

The results clearly show that as the balloon mission progresses, the prediction quality greatly increases. The largest change in prediction quality occurs immediately following balloon burst. After burst, the quality is within 3.53% of the total traveled range on average. This is a significant improvement over the initial prediction error of 36%. During actual missions in which the in-flight predictions were transmitted to the ground crew in real-time, this information was invaluable as it identified the landing location of payload

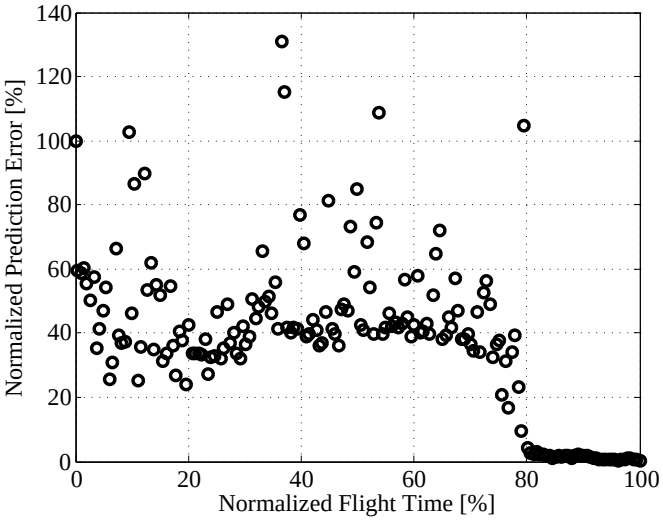

Figure 8: Landing location error calculated in real-time on-board the balloon-payload system for a high altitude mission.

systems to within 5km at only 60% of the total flight distance. This permitted ground teams to efficiently plan an approach to the recovery area early on, as well as maintain line of sight communications.

As the system uses collected information, it can eventually overcome any initial input errors. For example, if wind data are severely inaccurate (due to human error or poor forecast data), the system can overcome the poor data by collecting actual data during the ascent. In some scenarios this can cause the accuracy to degrade temporarily, as is the case with the low altitude tests 3 & 4 in Figure 5. Here the pre-flight predicted ascent rate was too high, and the predicted wind data set generally underestimated the actual wind. During ascent more accurate wind was collected as well as a better estimate of the actual ascent rate. This situation caused the predicted landing location to increase; however, the predicted burst altitude was higher than the actual by $2.15km$. This caused the predicted landing location error to increase as the payload got closer to balloon burst. After burst this error was remedied as the location of burst is no longer used in calculations.

Experimental flight testing validated the capacity for small microprocessor to perform the in-flight prediction updates. Although the system did not have the smoothing on the ascent and descent rate estimation, improved predictions were still generated. In the low altitude full flight testing the system was capable of significantly reducing the initial prediction error in flight tests 1 & 2. Flight tests 3 & 4 did not show a marked improvement until after balloon burst. This is due to the same situations as discussed previously for the simulated low altitude tests (as they used the same GPS data). The necessity for ascent rate smoothing is also clear in the high altitude full flight test. As the system was ascending very slowly ($3\ m/s$), differentiation of noisy GPS data produced highly noisy predicted landing location estimates. However, as with all tests, after balloon burst, the predicted landing location error quickly approaches zero.

The natural question arises whether the in-flight predictions are better simply because they are closer to the landing location. In order to test this, predictions were computed at the same time and location as the in-flight predictions; however, only pre-flight parameters were used. A typical simulation result is shown in Figure 9. Here it can be seen that the initial parameter predictions do indeed get better as the flight time increases; however, the in-flight predictions using the collected flight data decrease much faster than the predictions performed with initial characteristics. This result is typical for nearly all simulations tested.

VI. Conclusions

A hardware/software system has been developed to improve upon pre-flight predicted landing locations for a balloon mission by performing in-flight prediction updates using estimated flight parameters. Many factors impact the accuracy of a prediction including: ascent rate, descent rate, burst altitude, and forecast wind data. The system developed reduces the errors due to these factors in real-time on-board the balloon-payload system by measuring and updating these flight parameters.

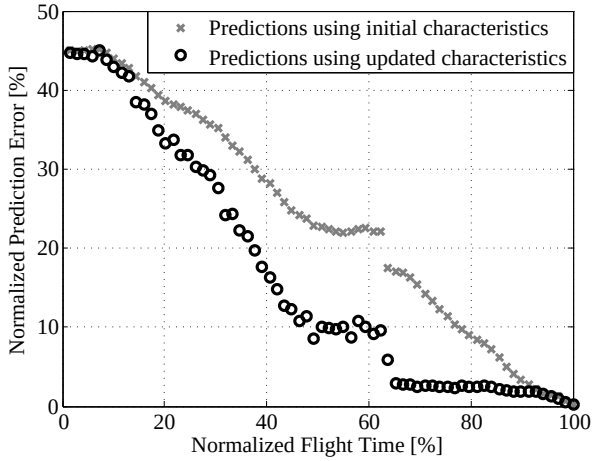

Figure 9: Landing location error computed at various points throughout the balloon mission using both initial and measured flight characteristics.

Improvements provided by the system are broken down into two phases; those improvements performed during ascent, and those performed during descent. During the balloon's ascent phase, the ascent rate is approximated using GPS data. Additionally, wind data is collected during the ascent replacing the pre-flight forecast wind data. After the balloon bursts, errors associated with predicting the burst altitude are no longer applicable. During the descent phase, updated winds from the ascent phase are used exclusively in estimating the wind conditions. Similar to the ascent phase, the descent rate (and the corresponding estimated drag coefficient) are approximated using GPS data during descent.

Results calculated by post-processing balloon GPS data demonstrate the benefit of continuously updating the prediction in-flight. Initial pre-flight predictions are accurate to only 36% of the total range traveled on average (using best estimates of the flight characteristics); however, at balloon burst the accuracy of the prediction has improved by nearly an order of magnitude (3.5% of the total range on average). Additional results have shown that measuring and estimating the flight characteristics in-flight does improve the prediction significantly over predictions computed using the pre-flight parameter values.

In-flight results computed during five balloon missions further validate the algorithm developed. Results also validated the capacity for the entire in-flight improvement algorithm to be performed on a small microprocessor and transmitted to the ground crew using existing radio communications.

Acknowledgements

Funding provided by the Nevada NASA Space Grant Consortium through NASA grant number NNX10AJ82H. Additionally, the authors would like to acknowledge Andrew Smith and George Kehagias for their participation and assistance in developing the hardware and performing flight tests.

T. Fields was supported by the National Science Foundation GK-12 Program, Grant DGE No. 1045584. Any opinions, findings, and conclusions or recommendations expressed in this material are those of the author(s) and do not necessarily reflect the views of the National Science Foundation.

References

[1]Baker, J. and Taylor, R., "Near-Space and the BAMASAT Program," *ASEE Southeastern Section Annual Conference*, Tuscaloosa, AL, April 2006.

[2]Palumbo, R., Morani, G., and Corraro, F., "Balloon Trajectory Prediction Methodologies for the Unmanned Space Vehicles Programme," *Proceedings of the 20th ESA Symposium on European Rocket and Balloon Programmes and Related Research*, Hyere, France, May 22-26, 2011.

[3]Palumbo, R., *A Simulation Model for the Trajectory Forecast, Performance Analysis and Aerospace Mission Planning with High Altitude Zero Pressure Balloons*, Ph.D. thesis, Universita Degli Studi Di Napoli "Federico II", November 2007.

[4]Palumbo, R., Mercogliano, P., Corraro, F., Matteis, P. D., and Sabatano, R., "Meteorological Conditions Forecast and

Balloon Trajectory Estimations," *Memorie della Societ Astronomica Italiana*, Vol. 79, 2008, pp. 841–845.

[5]Musso, I., Cardillo, A., Cosentino, O., and Memmo, A., "A Balloon Trajectory Prediction System," *Advances in Space Research*, Vol. 33, 2004, pp. 1722–1726.

[6]"Near Space Ventures Inc., Flight Track Prediction INPUT PAGE," Near Space Ventures Inc. Web. 1 Dec 2012. (http://nearspaceventures.com/w3Baltrak/readyget.pl).

[7]Fischer, J. and Kansaku, C., "Supplemental Instruction in Mathematics within a Mathematics/Software Engineering Co-Development Project to Dynamically PRedict High-Altitude Balloon Paths," *118th ASEE Annual Conference & Exposition*, Vancouver, B.C. Canada, June 26-29, 2011.

[8]Fields, T. D., LaCombe, J. C., and Wang, E. L., "Autonomous Guidance of a Circular Parachute Using Descent Rate Control," *Journal of Guidance, Control, and Dynamics*, Vol. 35, No. 4, 2012, pp. 1367–1370.